

INTERMEDIATE TEMPERATURE SOLID OXIDE FUEL CELL PERFORMANCE OPTIMISATION

Lionel COMBEMALE, Visweshwar SIVASANKARAN, Gilles CABOCHE

Laboratoire Interdisciplinaire Carnot de Bourgogne, UMR 6303 CNRS – Univ. Bourgogne Franche-Comté, BP 47870, 21078 Dijon, France

Abstract – The performances of anode-supported Intermediate Temperature-Solid Oxide Fuel Cells (IT-SOFC), obtained by tape casting, are investigated. The tested cells are composed of four layers: cathode, electrolyte, anode and Anode Functional Layer (AFL). The AFL has to ensure mechanical compatibility between anode and electrolyte and to increase the output power. First performance tests are conducted in the 500°C – 600°C temperature range to determine the maximum power density. In a second time, other parameters are investigated: cathode and electrolyte thickness. For each modification, the performance, in terms of power density, is measured. These results lead to the production of optimised cells which are used to realise long term ageing tests under working conditions. First reactivity results are then discussed.

Résumé – Optimisation des performances d’une pile à combustible à température intermédiaire. Les performances de cellules supportées anode pour piles à combustible à température intermédiaire de fonctionnement sont présentées. Ces cellules, obtenues par coulage en bande, sont composées de quatre couches: une cathode, un électrolyte, une anode et une couche fonctionnelle (Anode Functional Layer, AFL). L’AFL assure la compatibilité mécanique entre le composé anodique et l’électrolyte permettant d’accroître la puissance de sortie de la cellule. Dans un premier temps, des tests de performance sont menés entre 500°C et 600°C afin de déterminer la température de fonctionnement optimale. L’impact d’autres paramètres (épaisseur de la cathode et de l’électrolyte) est ensuite présenté. Pour chaque modification, les performances, en termes de densité de puissance, sont mesurées. Ces résultats conduisent à la production de cellules optimisées. Ces cellules optimisées sont finalement utilisées pour réaliser des essais de vieillissement dans les conditions de travail. Les premiers résultats de réactivité, obtenus suite à ces vieillissements de longue durée, sont présentés et discutés.

1. INTRODUCTION

In recent years, much effort has been devoted to developing intermediate temperature solid oxide fuel cells (IT-SOFCs) operating at 500–600 °C in order to improve the material compatibility, the durability and to reduce SOFC costs. However, the reduction of operating temperature is followed by a decrease in the electrochemical performance of each material constituting the “classical” solid oxide fuel cell. Therefore, the choice of the cell materials is restricted to those electrochemically active at this temperature range. Gadolinia-doped ceria ($Gd_{0.1}Ce_{0.9}O_2$) is a

Tirés-à-part : L. COMBEMALE, ICB, Université de Bourgogne, 21078 Dijon Cedex, France.

promising candidate for SOFCs electrolyte at intermediate temperatures thanks to its high ionic conductivity [1], its low activation energy and its chemical stability from room temperature to its melting point (approximately 2300 °C). D. J. L. Brett and al. have mentioned the thickness of electrolyte as a key point in improving the performance of the cells. By reducing the size layer of $\text{Gd}_{0.1}\text{Ce}_{0.9}\text{O}_2$ (GDC), the electrical performance could be kept constant even if the working temperature decreases. Considering electrical conductivity and performance working in the 500-600 °C temperature range, the electrolyte thickness must be lowered to 15-20 μm [2], in that case the electrical performance could reach $0.6 \text{ W}\cdot\text{cm}^{-2}$ [3]. For the cathode material, lanthanum strontium cobalt iron oxides, with the specific composition $\text{La}_{0.6}\text{Sr}_{0.4}\text{Co}_{0.2}\text{Fe}_{0.8}\text{O}_3$ (LSCF48), is largely used because of its active electro-catalytic properties in the working temperature range. Moreover, its thermal expansion coefficient is in accordance with the GDC electrolyte [4, 5]. To reduce polarization problems at the cathode side a mix between LCF48 and GDC is recommended. The mass ratio could be comprised between 50:50 and 70:30 for the cathode and the electrolyte materials [6, 7]. Even if new materials have recently been developed for the anode [7, 8], the Ni/GDC cermet shows excellent electrochemical performances in the case of the use of pure H_2 as a fuel [9].

Presently, IT-SOFC cells could be obtained by different techniques such as spin coating [10], chemical vapor deposition [11], dip coating [12] or screen printing [13]. These methods involve high initial capital costs and many steps of sintering at high temperature which increase the cost and time of fabrication and thus lead to costly processes. On the contrary, tape casting process was widely used to fabricate electronic devices [14, 15, 16] and is also an attractive process to obtain planar anode supporting SOFCs because of its low cost for mass production [17, 18, 19].

By following these investigations different IT-SOFC cells were realized following a patented process [20]. To increase the performances, these cells are composed of four layers: anode, electrolyte, cathode and an Anode Functional Layer (AFL). The AFL is normally used to maximize the three-phase boundary length and to restrain the activation polarization at the anode side [20].

The goals of this work are twofold. The first objective is to define the optimum temperature which permits to reach the maximum performances, in terms of power density, for these cells in the 500 °C – 600 °C temperature range. The second objective is focused on the optimization of the power performances based on cathode and electrolyte modification. Finally, ageing tests are conducted and performance degradation is explained in terms of morphology and structure modification.

2. EXPERIMENTAL PROCEDURE

2.1. Fuel cell preparation process

To obtain IT-SOFC unit cells the materials are selected based on their electrochemical properties in the temperature range 500 °C – 600 °C. Accordingly, for the cathode, a mix between the perovskite compound LSCF48 and the electrolyte GDC is used (respectively 65:35 mass ratio). LSCF48 is synthesized by solid state reaction [21] at the ICB laboratory. GDC (provided by Neyco) is used as well as electrolyte material and a mixture of NiO (Sigma-Aldrich 99.99 % purity) and GDC (Neyco) is used as anode material (respectively 65:35 mass ratio). The shaping process is realized by tape-casting by following the recommendations given in a previous patent [22]. Finally, rectangular cells with an active area equal to 10 cm^2 are obtained.

2.2 Electrical performance determination

The power density is measured by using an open flange set-up device. This commercial system, sold by Fiaxell, gives the opportunity to realize experimentations under real conditions. Indeed, its design allows the introduction of different gases at the anode and the cathode side. NiO foam coated with NiO powders are used as anode current collector and gold grid is used as cathode current collector. Heating of the cell is started with air on both sides. The electrochemical performances are measured with air as oxidant and fuel starting with N_2/H_2 (92/8) gas mixture then replaced, step by step during the experiments, by humidified hydrogen (3 vol.% at room temperature). During the experiment hydrogen and air flow rates are kept constant at 210 and 600 $ml\ min^{-1}$. NiO in the anode layers is then totally reduced to Ni during the hydrogen flow [21].

2.3 Structural and microstructural characterizations

All the presented cell pictures are realized using scanning electron microscopy Hitachi SUI 510. The reactivity between electrolyte and electrodes is characterized by using an X-ray diffractometer (D5000 X-Ray diffractometer, $CuK_{\alpha 1}$, θ - 2θ mode) at a scanning rate of $1.2\ ^\circ.min^{-1}$ and a $58^\circ < 2\theta < 85^\circ$ range. The obtained diffraction diagrams are treated by EVA software to determine the nature of the observed microstructures.

3. EXPERIMENTAL RESULTS

3.1. Impact of different parameters on cell performance

3.1.1. Working temperature influence. Different I-V curves are realized between 500 °C and 600 °C with a temperature step equal to 25 °C. The objective is to determine the best working temperature in terms of power density. The maximum power density is then determined by drawing the $P = f(I)$ curves (*figure 1a*). *Figure 1b* compiles all these results by showing P_{max} versus Temperature. The OCV values decrease from 1.04V at 500 °C to 0.92 V at 600 °C. This can be explained by the Gibbs free energy formation of the water which tends to be less negative at high temperature. The OCV value, measured in this temperature range, is closed to the theoretical one and demonstrates that there are no leakages between the anode and cathode compartments.

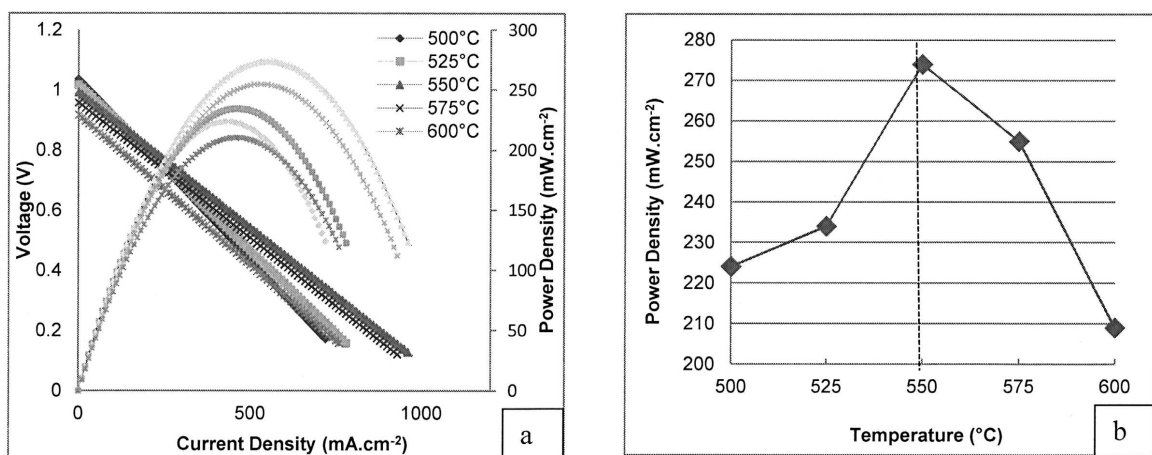
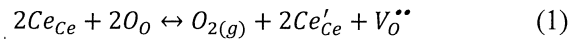


Figure 1. Temperature impact on the electrical performance a) electrochemical curves at different temperatures b) Maximum power density obtained at different temperatures.

The cell exhibits a maximum power density of 274 mW.cm^{-2} at $550 \text{ }^\circ\text{C}$. Below this temperature, the measured power is lower. Indeed, O^{2-} ionic diffusion is thermally activated and its diffusion coefficient follows an Arrhenius law. So, the O^{2-} diffusion coefficient value decreases with the temperature.

Above 550°C , the cerium reduction can be observed in reductive atmosphere. This has been demonstrated by RV Wandekar [23] and can be explained by the following *reaction 1* (in Kröger-Vink nomenclature):



The presence of Ce^{3+} in the GDC crystallographic structure leads to electronic conduction apparition between Ce^{4+} and Ce^{3+} . Thus, the electrolyte loses its insulator role and the performance is degraded.

3.1.2. Electrolyte layer influence. The electrochemical performances are correlated to the electrolyte thickness. The electrolyte layer has to be as thin as possible to reduce the length to cross for ionic oxygen. However, there are two limits concerning the electrolyte size. The first one is related to the shaping technique. Indeed, by using tape casting it is not possible to obtain a thickness below $10 \mu\text{m}$ after sintering. To produce thinner layers, physical deposition methods have to be employed. The second limit concerns the minimum thickness for the electrolyte to insure its insulating role. Below 1 or $2 \mu\text{m}$, short circuits may occur between anode and cathode. By following these limits, two cells are produced, with an electrolyte thickness equal to $20 \mu\text{m}$ and $40 \mu\text{m}$. For each cell, the size and morphology of the electrodes are kept constant.

Figure 2 presents the electrochemical tests realized on each cell. The OCV (Open Circuit Voltage) measurements give two close values: 911 mV for $20 \mu\text{m}$ and 920 mV for $40 \mu\text{m}$. That means there is no leakage in the electrolyte and no hydrogen can be in direct contact with oxygen. As expected, the maximum power density is obtained for an electrolyte thickness equal to $20 \mu\text{m}$. In this case, the maximum power density reached is 227 mW.cm^{-2} .

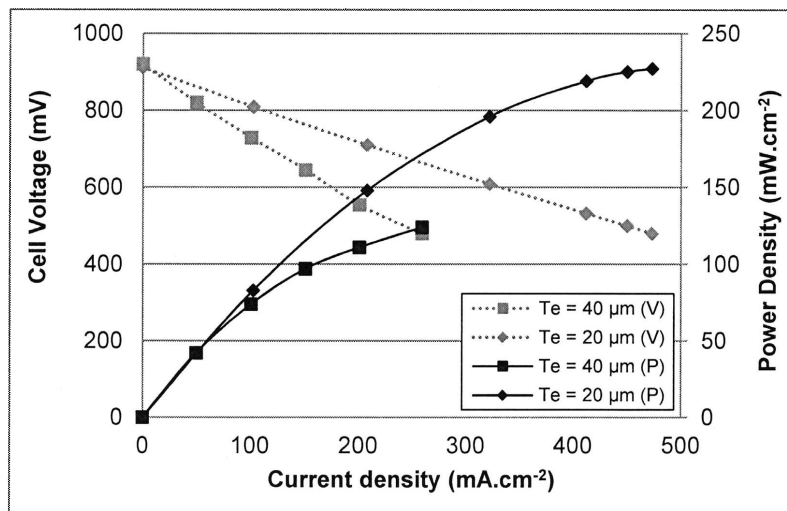


Figure 2. Electrochemical tests realized on two different cells – Electrolyte layer: 20 and $40 \mu\text{m}$. Dashed lines correspond to Cell Voltage vs Current Density. Full lines correspond to Power Density vs Current Density

3.1.3. Cathode layer influence. The same kinds of experimentations are conducted to determine the thickness influence of the cathode layer. In this case, two cells are produced with a cathode thickness equal to 10 μm (called: T_{c10}) and 50 μm (called: T_{c50}). For each cell, the electrolyte and the anode present the same size and the same morphology.

Figure 3 presents the electrochemical tests realized on each cell. The OCV measurements give an expected value for T_{c50} : 911 mV. In contrast, for T_{c10} the measured value is very low: 862 mV. Similar observations can be made for the maximum power density. Indeed, even if for T_{c50} the maximum power density reached 227 $\text{mW}\cdot\text{cm}^{-2}$ for T_{c10} this value does not exceed 81 $\text{mW}\cdot\text{cm}^{-2}$. OCV degradation observed for T_{c10} can be explained by two different factors: presence of porosity in the electrolyte layer or reduction of Ce^{4+} contained in GDC10. SEM observations (not presented here) are conducted to check the electrolyte morphology. No trough-porosities are detected. So, the low performances are not due to a direct contact between hydrogen and air. Concerning Ce^{4+} reduction, as it is explained in section 3.1.1., the electrolyte is very sensitive to reductive atmosphere. The reduction reaction, which conducts to Ce^{3+} formation and electronic conduction, is driven by temperature and atmosphere composition. In this part, the anode material and thickness and the working temperature are similar for T_{c10} and T_{c50} . So, thermodynamic conditions are the same in the two cases and cannot explain the low OCV values. Finally, an explanation may be found by considering the electrochemical test bench. A thicker cathode layer can improve the seal integrity during the measurements [24].

For the maximum power density evolution, these experimentations show a relation between maximum power density and cathode size layer. A thicker cathode layer presents a large amount of Triple Phase Boundary (TPB). By considering the pathway model [25], this leads to a better integration of ionic oxygen in the electrolyte and gives better performances.

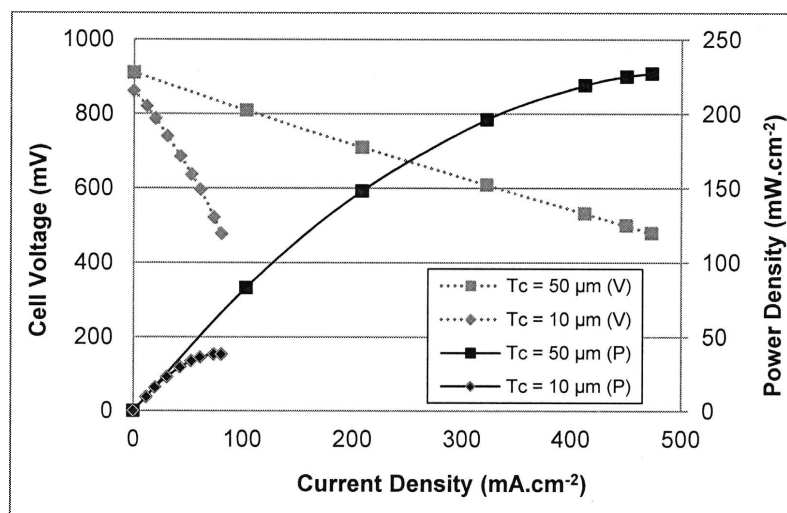


Figure 3. Electrochemical tests realized on two different cells – Cathode layer: 10 and 50 μm . Dashed lines correspond to Cell Voltage vs Current Density. Full lines correspond to Power Density vs Current Density

3.1.4. Optimized cell morphology. By following the previous observations, a complete optimized cell is produced. Figure 4 shows a SEM picture of this cell. It is composed of four layers: cathode

(thickness around 50 μm), electrolyte (thickness around 20 μm), Anode Functional Layer (around 30 μm) and anode (around 300 μm).

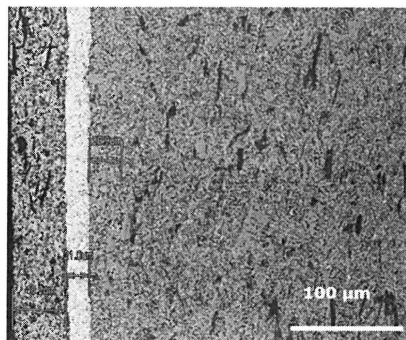


Figure 4. SEM picture of an optimized cell.

3.2. Long term ageing tests results

The cell produced by following the optimized morphology is then used for long term ageing tests. This experimentation consists in placing the cell in real working conditions and in following the power density evolution. This test is stopped after 133h when 10 % of the initial power density value is lost. Analyses realized on the cathode and electrolyte parts show no modification on either the morphology or the microstructure.

On the contrary, the anode is largely modified. Some cracks are visible by SEM observations (*figure 5*). These cracks can conduct to performance degradation by changing the atmosphere at the AFL/electrolyte interface. Indeed, a large amount of hydrogen gas can place GDC10 in a reductive atmosphere and lead to Ce^{3+} formation.

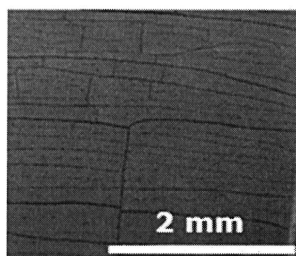


Figure 5. SEM picture realised on the anode side after 133h under working conditions.

XRD analysis is then realised on the anode side (*figure 6*). Before ageing test, NiO and GDC10 are clearly visible. These compounds are expected due to the fabrication process. After ageing test GDC10 is detected as well as Ni which is formed after NiO reduction. Nevertheless, an unwanted phase is observed at 37° and 43° : NiO. As explained in section 2.2. during the experimentation all NiO is reduced under Ni form during the increasing temperature step. Apparition of NiO can cause cracks appearance because its lattice parameter (4.178 \AA) is larger than that of pure Ni (3.53 \AA).

Oxygen that integrates Ni metallic structure, to form NiO, comes from the electrolyte and due to low H_2 gas concentration can react with Ni. One way to avoid the appearance of cracks could be to change the pore-former, to form larger porosities, or to increase the pore-former amount, to increase the number of porosities.

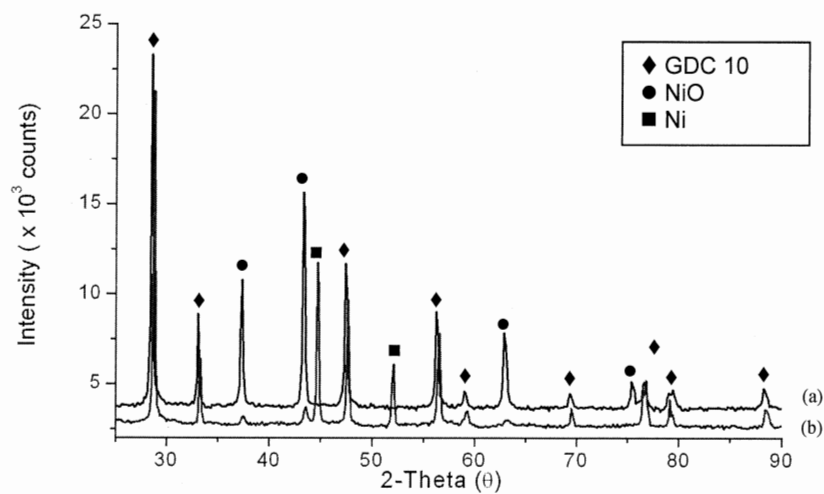


Figure 6. XRD pattern obtained on the anode side before (a) and after (b) ageing test under working conditions.

4. CONCLUSIONS

The electrical performances of Intermediate Temperature Solid Oxide Fuel Cells are optimized by studying the influence of the working temperature and the impact of the thickness of the cathode and the electrolyte. It has been demonstrated that the optimum working temperature is 550°C. This allows to increase ionic oxygen diffusion and to prevent formation of Ce^{3+} . As expected, better results are obtained for a thin electrolyte layer (20 μm). However, a surprising observation has been made for the cathode. Indeed, a thicker cathode layer (50 μm) gives a higher power density. Actually, the reason for this observation is not really well understood and could be due to the electrochemical test bench. By following all of these results a maximum power density of 227 $mW.cm^{-2}$ is achieved. At end, one optimized cell is produced to realize ageing test under working condition. After 133 h, the power density has lost 10 % of its initial value. This performance degradation is due to NiO appearance in the anode part and to direct contact between electrolyte and H_2 gas.

5. REFERENCES

- [1] B.C.H. Steele, A. Heinzel, Materials for fuel-cell technologies, *Nature* 414 (2001) 345-352.
- [2] D. J. L. Brett, A. Atkinson, N. P. Brandon, S.J. Skinner, Intermediate temperature solid oxide fuel cells, *Chem. Soc. Rev.* 37 (2008) 1568-1578.
- [3] C. Ding, H. Lin, K. Sato, K. Amezawa, T. Kawada, J. Mizusaki, T. Hashida, Effect of thickness of $Gd_{0.1}Ce_{0.9}O_{1.95}$ electrolyte films on electrical performance of anode-supported solid oxide fuel cells, *J. Power Sources* 195 (2010) 5487-5492.
- [4] V.V. Kharton, F.M. Figueiredo, L. Navarro, E.N. Naumovich, A.V. Kovalevsky, A.A. Yaremchenko, A.P. Viskup, A. Carneiro, F.M.B. Marques, J.R. Frade, Ceria-based materials for solid oxide fuel cells, *J. Mat. Sciences* 36 (2001) 1105-1117.

- [5] K. Świerczek, Thermoanalysis, nonstoichiometry and thermal expansion of $\text{La}_{0.4}\text{Sr}_{0.6}\text{Co}_{0.2}\text{Fe}_{0.8}\text{O}_{3-\delta}$, $\text{La}_{0.2}\text{Sr}_{0.8}\text{Co}_{0.2}\text{Fe}_{0.8}\text{O}_{3-\delta}$, $\text{La}_{0.9}\text{Sr}_{0.1}\text{Co}_{1/3}\text{Fe}_{1/3}\text{Ni}_{1/3}\text{O}_{3-\delta}$ and $\text{La}_{0.6}\text{Sr}_{0.4}\text{Co}_{0.2}\text{Fe}_{0.6}\text{Ni}_{0.2}\text{O}_{3-\delta}$ perovskites, *Solid State Ionics*, 179 (2008) 126-130.
- [6] V. Dusastre, J. A. Kilner, Optimisation of composite cathodes for intermediate temperature SOFC applications, *Solid State Ionics* 126 (1999) 163-174.
- [7] E. Perry Murray, M.J. Sever, S.A. Barnett, Electrochemical performance of (La,Sr)(Co,Fe)O₃–(Ce,Gd)O₃ composite cathodes, *Solid State Ionics* 148 (2002) 27-34.
- [8] R. Martinez-Coronado, J.A. Alonso, M.T. Fernandez-Diaz, $\text{SrMo}_{0.9}\text{Co}_{0.1}\text{O}_{3-\delta}$: A potential anode for intermediate-temperature solid-oxide fuel cells (IT-SOFC), *J. Power Sources* 258 (2014) 76-82.
- [9] A. Azzolini, J. Downs, V.M. Sglavo, Fabrication and co-sintering of thin tubular IT-SOFC with Cu₂O–GDC cermet supporting anode and Li₂O-doped GDC electrolyte, *J. Eur. Ceram. Soc.* 35 (2015) 2119-2127.
- [10] R.V. Wandekar, M. Ali-Basu, B.N. Wani, S.R. Bharadwaj, Physicochemical studies of NiO–GDC composites. *Mat. Chem. Phys.* 99 (2006) 289-294.
- [11] B.C.H. Steele, Fuel-cell technology: Running on natural gas, *Nature* 400 (1999) 619-621.
- [12] K. Joon, Fuel cells – a 21st century power system, *J. Power Sources* 71 (1998) 12-18.
- [13] Y. J. Leng, S. H. Chan, K. A. Khor, S. P. Jiang, P. Cheang Effect of characteristics of Y₂O₃/ZrO₂ powders on fabrication of anode-supported solid oxide fuel cells, *J. Power Sources* 117 (2003) 26-34.
- [14] M. Letilly, O. Joubert, M. Caldes, A. Le Gal La Salle, Tape casting fabrication, co-sintering and optimisation of anode/electrolyte assemblies for SOFC based on BIT07-Ni/BIT07, *Int. J. Hydrogen Energy* 37 (2012) 4346-4355.
- [15] T.L. Ren, H.J. Zhao, L.T. Liu, Z.J. Li, Piezoelectric and ferroelectric films for microelectronic applications, *Mater. Sci. Eng. B* 99 (2003) 159-163.
- [16] W. Tavernor, H.P.S. Li, A.J. Bell, R. Stevens, Improved Compaction in Multilayer Capacitor Fabrication, *J. Eur. Ceram. Soc.* 19 (1999) 1691-1695.
- [17] L.F.G. Setz, I. Santacruz, M.T. Colomer, S.R.H. Mello-Castanho, R. Moreno, Tape casting of strontium and cobalt doped lanthanum chromite suspensions, *J. Eur. Ceram. Soc.* 30 (2010) 2897-2903.
- [18] J.-H. Myung, H.J. Ko, H.G. Park, M. Hwan, S.H. Hyun, Fabrication and characterization of planar-type SOFC unit cells using the tape-casting/lamination/co-firing method, *Int. J. Hydrogen Energy* 37 (2012) 498-504.
- [19] S. Beaudet Savignat, M. Chiron, C. Barthet, Tape casting of new electrolyte and anode materials for SOFCs operated at intermediate temperature, *J. Eur. Ceram. Soc.* 27 (2007) 673-678.
- [20] K. Chen, X. Chen, Z. Lu, N. Ai, X. Huang, W. Su, Performance of an anode-supported SOFC with anode functional layers, *Electrochimica Acta* 53 (2008) 7825-7830.
- [21] V. Sivasankaran, L. Combemale, M.C. Péra, G. Caboche. Initial Preparation and Characterization of Single Step Fabricated Intermediate Temperature Solid Oxide Fuel Cells (IT-SOFC), *Fuel Cells* 14 (2014) 533-536.
- [22] V. Sivasankaran, L. Combemale, G. Caboche, Procédé de préparation d'une pile à combustible, French Patent n°WO 2014057218 A2.
- [23] R.V. Wandekar, M. Ali (Basu), B.N. Wani, S.R. Bharadwaj, Physicochemical studies of NiO–GDC composites, *Mat. Chem. Phys.* 99 (2006) 289–294.
- [24] H. Xiao, T. Reitz, Anode-Supported Solid Oxide Fuel Cells with Thin Film Electrolyte for Operation at Reduced Temperatures, *ECS Transactions* 1 (2008) 201-208.
- [25] H. A. Taroco, J. A. F. Santos, R. Z. Domingues and T. Matencio, *Advanced in Ceramics – Synthesis and Characterisation, Processing and specific Applications*. Intech, 2011.

(Article reçu le 01/10/2015, sous forme définitive le 07/01/2016).